Effects of vertical reinforcement and boundary beam on the shear strength of RC wall located above an open frame

H. Shobu, M. Teshigawara & A. Nakamura
Nagoya University, Nagoya, Japan

N. Izumi, K. Matsumoto, T. Ichinose, S. Takahashi & S. Takakoshi
Nagoya Institute of Technology, Nagoya, Japan

T. Kamiya
Yahagi Construction Co., Ltd, Nagoya, Japan

H. Fukuyama
Building Research Institute, Tsukuba, Japan

H. Suwada & T. Kabeyasawa
National Institute for Land and Infrastructure Management, Tsukuba, Japan

SUMMARY:
Many RC structures were damaged in Kobe (1995) and Northridge (1994) Earthquakes. Especially, the damages of the buildings with open frames in the first story were severe. Therefore, current designers tend to provide strong walls in some frames that can resist most of the seismic force in the first story while leaving the remaining frames open. However, the shear strength of a wall located above an open frame may be smaller than that of a wall located above a stiff foundation. To investigate the effects of vertical reinforcement and boundary beam on the shear strength, four specimens with a two-story wall located above an open one-bay frame are tested. As a result, the effect of vertical reinforcement on the shear strength was larger than that of boundary beam. In addition, a method to evaluate the strength of the shear wall is proposed in this paper.

Keywords: RC, shear wall, boundary beam, vertical reinforcement, compression strut

1. INTRODUCTION

Apartment buildings often have stiff walls in the transverse direction in the upper stories and an open frame in the first story for the sake of a parking lot. Damages of such buildings were severe in Kobe (1995) and Northridge (1994) Earthquakes. To prevent such damages, current designers tend to provide strong walls in some frames that can resist most of the seismic force in the first story while leaving the remaining frames open. However, the behaviour of walls located above an open frame is not clear.

In general, loading test for RC shear wall is conducted with a wall located above a stiff foundation. Therefore, present methods to evaluate the shear strength of shear walls may not apply to shear walls above an open frame. The shear strength of a wall located above an open frame may be smaller than that of a wall located above a stiff foundation, because the confinements of wall deformations by a boundary beam of an open frame is smaller than that by a stiff foundation. On the other hand, vertical reinforcement in a wall panel constrains vertical deformations of a wall panel. Therefore, increasing vertical reinforcement in a wall panel may be equivalent with increasing the rigidity of the boundary beam. In this research, four specimens which have a two-story wall located above an open one-bay frame are tested to investigate the effect of vertical reinforcement and a boundary beam on the shear strength of such a wall. In addition, a method to evaluate the strength of the shear wall is proposed in this paper.

2. EXPERIMENTAL PROGRAM

2.1. Specimens

The reinforcement arrangement and the cross sections of the specimens used in this research are shown in Figs. 2.1 and 2.2, respectively. The reinforcement bar ratios are also indicated.

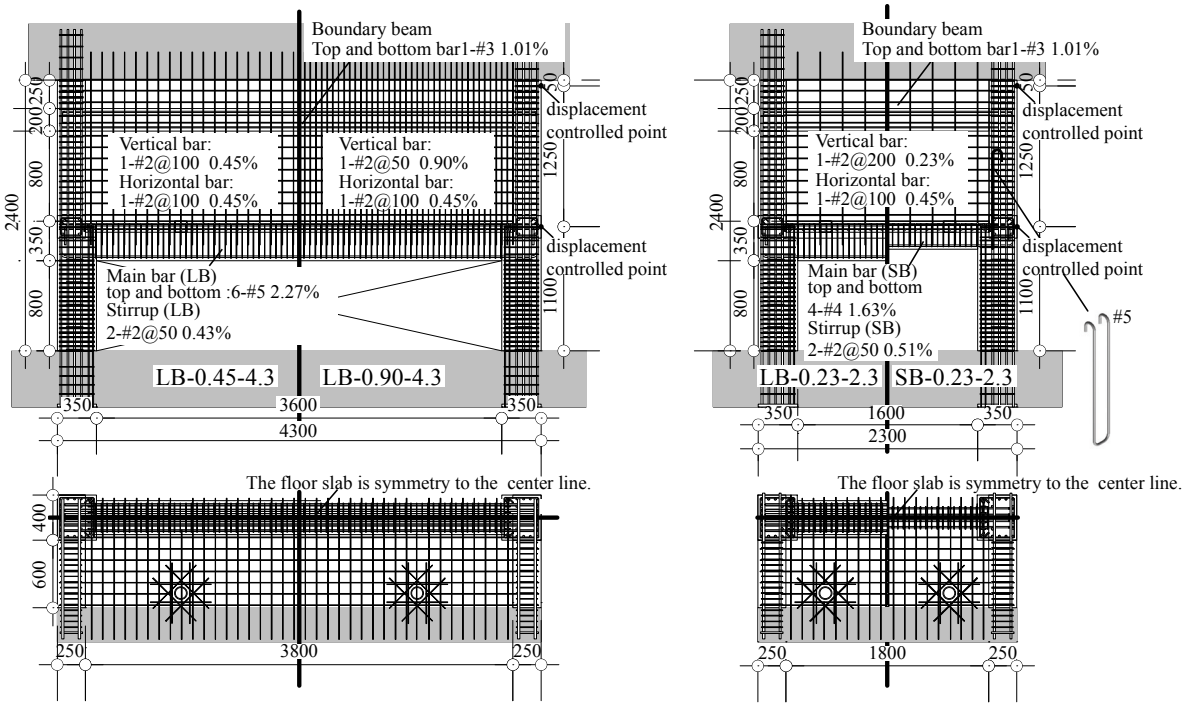

Figure 2.1. Reinforcement arrangement of specimens

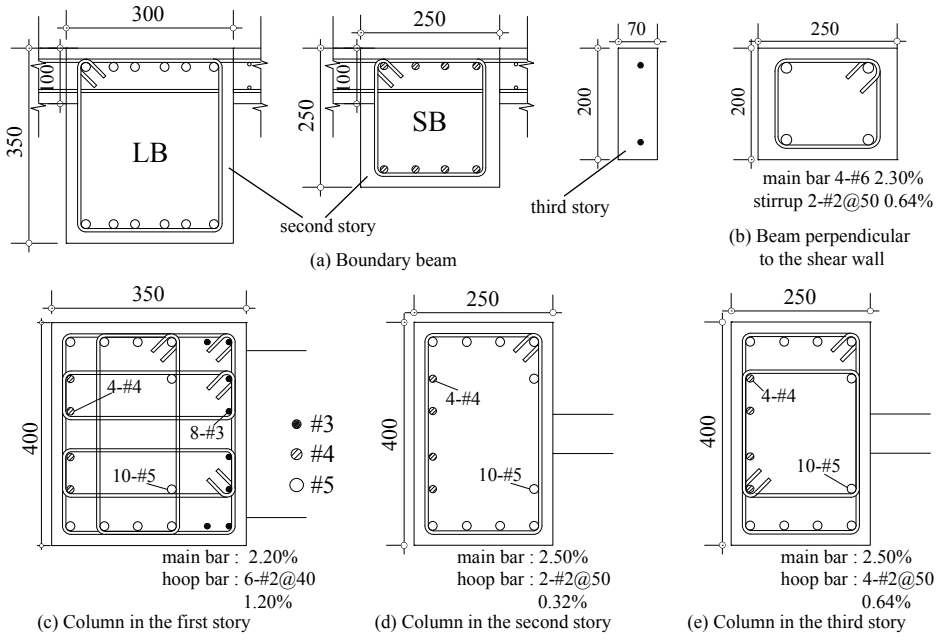

Figure 2.2. Cross sections of the columns and the boundary beam

The specimens were modeled at a scale of 1/3 of an existing building and represented the lower three-story of medium-rise RC building with an open frame in the first story. Four specimens were prepared in order to investigate the shear strength of wall located above an open frame. Each specimen had a two-story wall located above an open one-bay frame. Floor slabs were also constructed at the top of the open frame. The letters in specimen's name, LB or SB shows the size of the boundary beam

(Fig. 2.2 a). The former numbers of specimen's name, 0.23, 0.45 and 0.90 represent the ratio of vertical reinforcement in the wall panel. The latter numbers of specimen's name, 2.3 and 4.3 represent the span length of specimens. Table 2.1 summarizes the test parameters.

Table 2.1. Parameters of specimens

Specimen	Cross Section of Boundary Beam b×D (mm)	Ratio of vertical reinforcement of the wall panel p_{wv} (%)	Span length (m)
LB-0.45-4.3	300×350	0.45	4.3
LB-0.90-4.3		0.90	
LB-0.23-2.3		0.23	2.3
SB-0.23-2.3	250×250		

Two of the specimens have the short span (LB-0.23-2.3, SB-0.23-2.3). One of them has the large boundary beam (300 × 350 mm), and the other has the small boundary beam (250 ×250 mm). The remaining two specimens have the long span (LB-0.45-4.3, LB-0.90-4.3). One of them has the lower ratio of vertical reinforcement (0.45%), and the other has the higher ratio of vertical reinforcement (0.90%). All specimens were designed so that shear failure occur at the shear wall in the second story. The shear to flexural capacity ratios of the shear wall were approximately 0.67, where the flexural and shear capacities of the shear wall were calculated based on the guidelines by Building Center of Japan (2007). The reinforcement and concrete used in the specimens were tested and the results are shown in Table 2.2.

Table 2.2. Material properties of the specimens

Reinforcement				
Bar	f_y (N/mm²)	ε_y (μ)	E_s (N/mm²)	f_u (N/mm²)
#2 (D6)	419	2223	1.96×10^5	508
#3 (D10)	393	2372	1.87×10^5	552
#4 (D13)	406	2172	1.87×10^5	566
#5 (D16)	375	2135	1.86×10^5	558

Concrete		
Used area	F_c (N/mm²)	E_c (N/mm²)
First story	29.9	2.97×10^4
Second and Third story	29.0	2.45×10^4

2.2. Test Setup

Figure 2.3 shows the test setup. Lateral forces were applied at the top of the third story and at the slab. The forces were controlled so that the lateral drift angle in the first story was the same as that in the second story to prevent story collapse at the first story. Loading was repeated in positive and negative directions alternately. Loading was applied one cycle each at the lateral drift angle of R=±1/2000(rad.), ±1/1000, ±1/100, ±1/75, ±1/50, ±1/33, two cycles each at ±1/500, ±1/250, ±1/150. The axial force was applied to the top of the columns in the second story (Fig. 2.3). The amount of the axial force was approximately 20% of the axial capacity of the column in the first story (N=588kN).

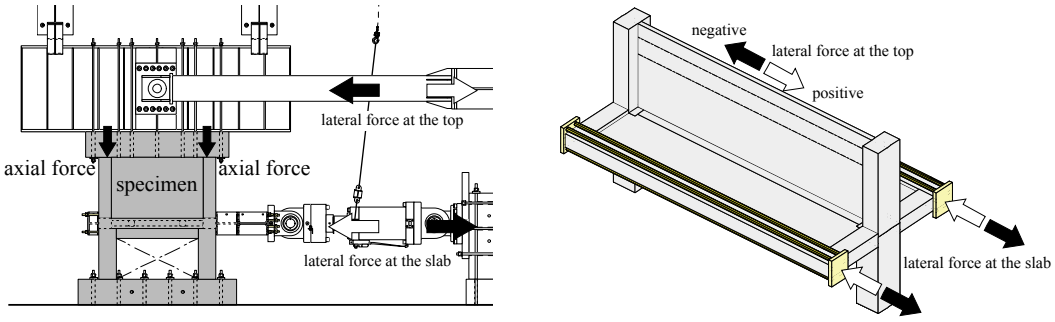

Figure 2.3. Test setup

Fig. 2.4 (a) shows the instrumentation arrangement of the linear variable differential transducers (LVDTs). There were three kinds of LVDTs. The first group measured the lateral displacement and is shown by the red color. The second group shown by the blue color measured the expansion and

contraction of the columns and the boundary beam. The last group shown by the green color measured the deflection of the boundary beam. Fig. 2.4 (b) shows the instrumentation arrangement of the strain gauges.

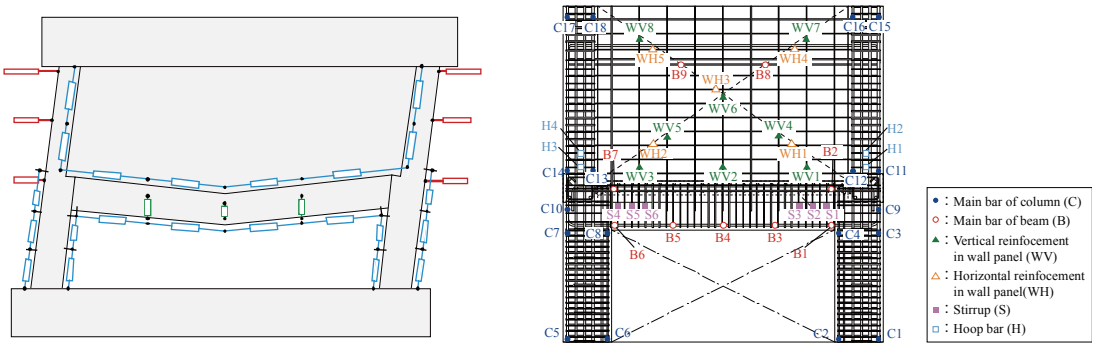

(a) LVDTs (b) Strain gauges

Figure 2.4. Instrumentation arrangement

3. TEST RESULT

3.1. Hysteresis Characteristics and Observed Damage

The relationships between the force at the top of the third story and the lateral drift angle of the specimens and the drift angles at which the reinforcement yielded are shown in Fig. 3.1.

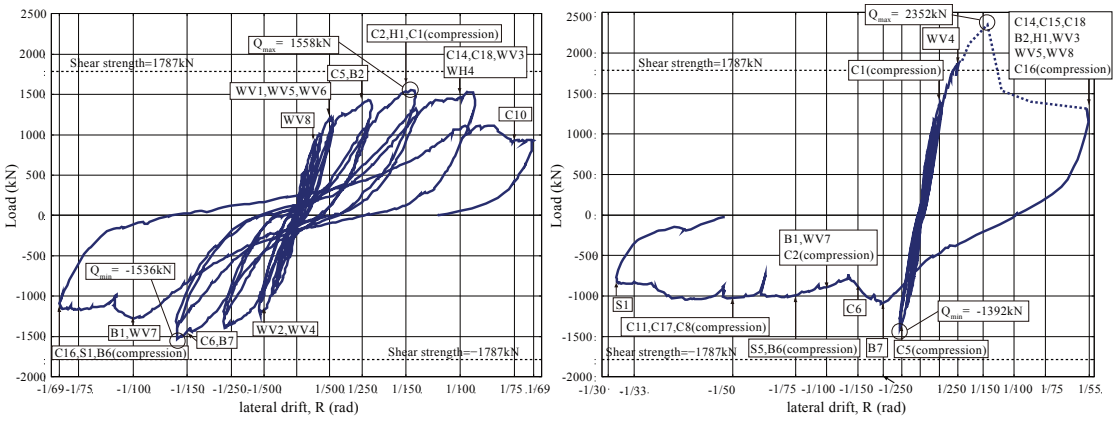

(a) LB-0.45-4.3 (b) LB-0.90-4.3

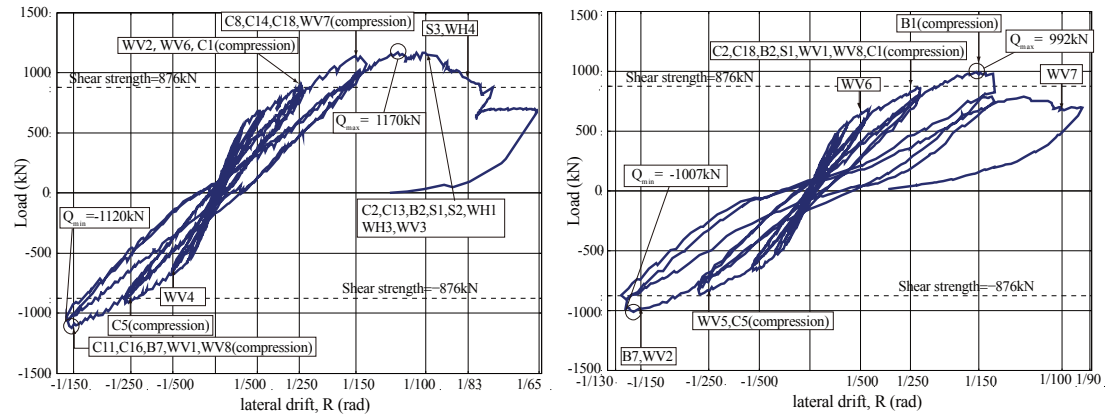

(c) LB-0.23-2.3 (d) SB-0.23-2.3

Figure 3.1. Lateral force – lateral drift angle relationship

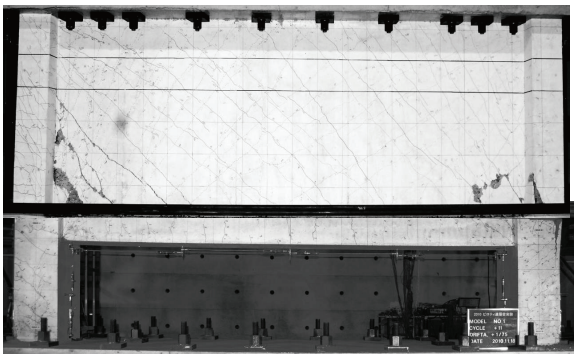

(a) LB-0.45-4.3

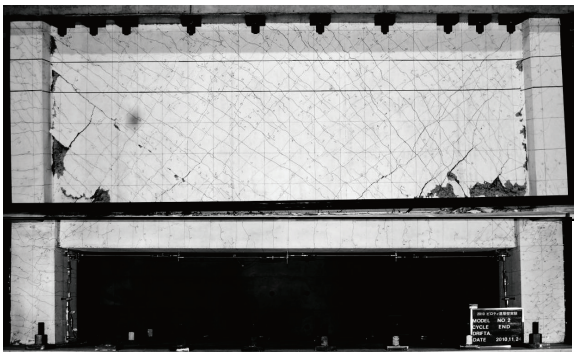

(b) LB-0.90-4.3

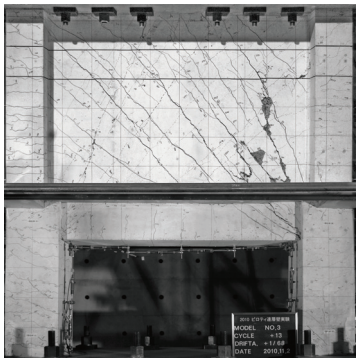

(c) LB-0.23-2.3

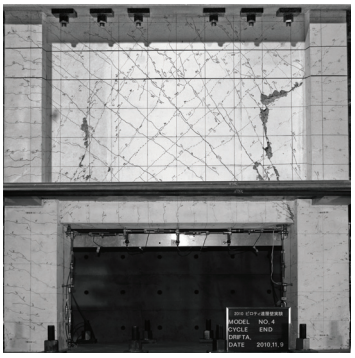

(d) SB-0.23-2.3

Figure 3.2. Final crack patterns in specimens

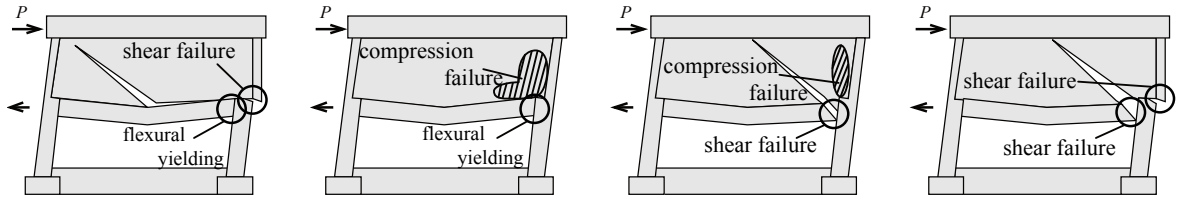

(a)Failure mode FS (b)Failure mode FC (c)Failure mode SC (d)Failure mode SS

Figure 3.3. Failure modes

The broken line in Fig. 3.1 shows the shear strength calculated according to the guidelines by Building Center of Japan (2007). The final crack patterns of the specimens are shown in Fig. 3.2.

In LB-0.45-4.3 (Fig. 3.1 a), the lateral force remained on the same level approximately after the top of main bar of the boundary beam (B2) yielded during cycle R = 1/250. During the same cycle, horizontal slip occurred between the wall panel and the boundary beam. The maximum strength (1558kN) was recorded at R = 1/155 after the hoop bar (H1) yielded. This value was below the shear strength (1787kN) calculated according to the guidelines by Building Center of Japan (2007). At the final stage, the horizontal slip between the wall panel and the boundary beam increased and the shear failure occurred at the bottom of the boundary column in the second story. This failure mode is shown in Fig. 3.3 (a).

In LB-0.90-4.3 (Fig. 3.1 b), shear cracks appeared in the wall panel during cycle R = 1/2000 and in the corner area of the boundary beam during cycle R = 1/1000. During cycle R = 1/500, flexural cracks appeared in the boundary column in the second story. Subsequently, the horizontal displacement of the top of the third story increased till R = +1/56 by the bungle of actuator control. The broken line in Fig. 3.1 (b) is solved by the data recorded with the actuator. At R = +1/141, the maximum strength (2353kN) was recorded. The maximum strength of LB-0.90-4.3 was 1.5 times of that of LB-0.45-4.3.

At the final stage, the corner area of the boundary beam in the second story yielded and compression failure occurred in the wall panel. This failure mode is shown in Fig. 3.3 (b).

In the short-span specimens (Fig. 3.1 c and d), the shear cracks in the wall panel extended toward the corner area of the boundary beam (Fig. 3.2 c and d). The maximum strengths of LB-0.23-2.3 and SB-0.23-2.3 were recorded at R = 1/120 and at R = 1/150 respectively, after the stirrup (S01) yielded. These strengths exceeded the shear strengths calculated according to the guidelines by Building Center of Japan (2007). The maximum strength of LB-0.23-2.3 was 1.2 times of that of SB-0.23-2.3. At the final stage, shear failure occurred at the corner area of the boundary beam in the second story and compression failure occurred in the wall panel. This failure mode is shown in Fig. 3.3 (c). In the short-span specimens, the horizontal slip did not occur between the wall panel and the boundary beam.

3.2. Discussion of the Results

Figure 3.4 shows the crack patterns of LB-0.45-4.3 and LB-0.23-2.3 at the peak of the shear strength during the positive loadings. The cracks in Fig. 3.4 appeared during the positive loading. In the long-span specimens (Fig. 3.4 a), the shear cracks in the area shown by red color appeared at a uniform angle. However, the angle of the shear cracks in the area shown by blue color was larger than that in the red color area. In the short-span specimens (Fig. 3.4 b), the shear cracks in the red color area appeared at 45 degrees approximately. However, the angle of the shear cracks in the blue color area was larger than 45 degrees. The cracks in the area shown by gray color are less than other areas of the wall panel.

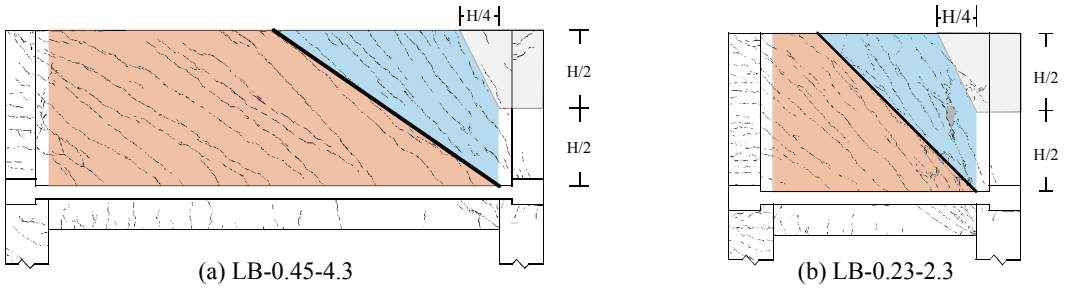

(a) LB-0.45-4.3 (b) LB-0.23-2.3

Figure 3.4. Crack patterns at positive peak loads

Figure 3.5 shows the strains distribution along the bottom bars in the boundary beam of LB-0.45-4.3 and LB-0.90-4.3 during the positive loadings. These specimens were measured the similar distributions of the strains and the bottom bars in the boundary beam did not yield before the maximum strength was recorded. The strains of LB-0.45-4.3 were larger than those of LB-0.90-4.3, because the vertical reinforcement of LB-0.45-4.3 was less than that of LB-0.90-4.3.

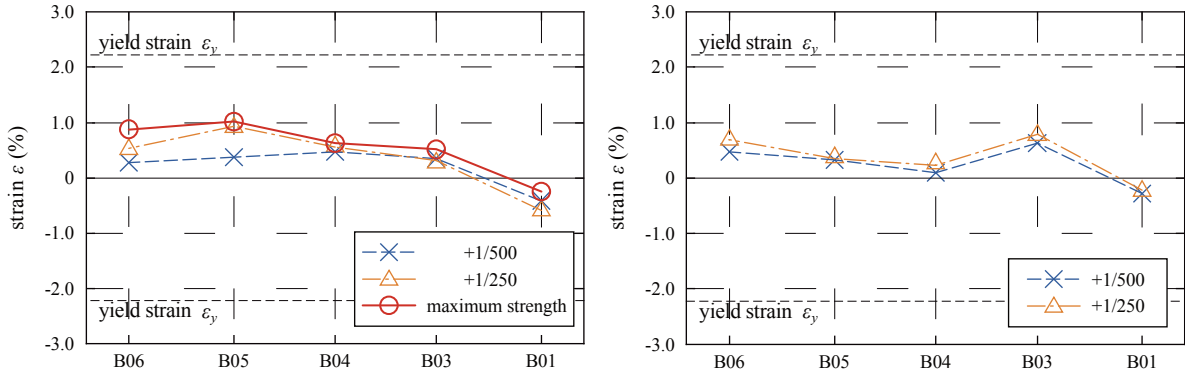

(a) LB-0.45-4.3 (b) LB-0.90-4.3

Figure 3.5. Strains distribution along the bottom bars in the boundary beam

The deformed shapes recorded with LVDTs at the peak of the shear strength during the positive loadings are shown in Fig. 3.6. The ratios shown in Fig. 3.6 indicate the tensile strains of the wall panel and the circle shown in Fig. 3.6 indicate the measurement position of LVDTs (Fig. 2.4 (a)). The vertical deformations of the wall panel are calculated from the rotation of the upper story and the deflection of the boundary beam. The tensile strains shown in Fig. 3.6 are calculated as the ratio of the vertical deformations to the height of the shear wall (1250mm). The tensile strains of the wall panel are as large as the yield strains of the vertical reinforcement in the wall panel approximately.

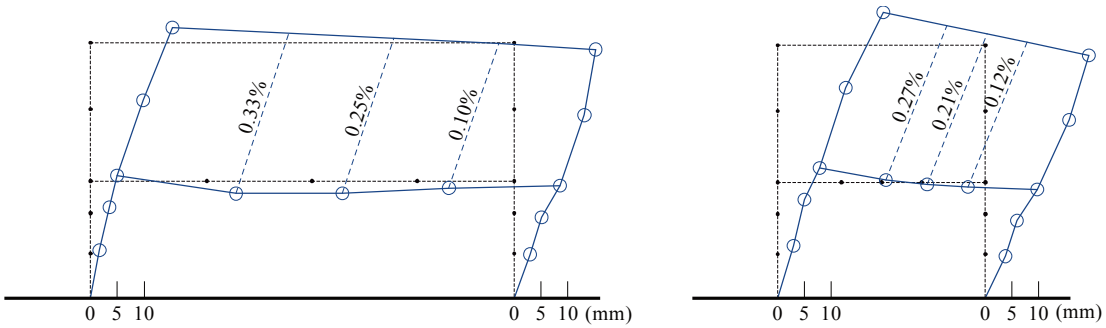

(a) LB-0.45-4.3 (b) LB-0.23-2.3

Figure 3.6. Deformed shapes at the peak of the positive loadings

4. ANALYSIS

Figure 4.1 shows the failure mechanism based on the observed damages. Lateral force applied to the shear wall is assumed to be resisted by C_1, C_2 and C_3 compression struts. Because C_1 and C_2 struts are connected to the boundary beam, they cause flexural yielding or shear failure at the corner of the boundary beam. C_3 strut cause compression failure at the wall panel or shear failure at the bottom of the boundary column, because it is connected to the boundary column. Additionally, the failure mode SS in Fig. 3.3 (d) could be considered to occur from the failure mechanism, although it was not observed.

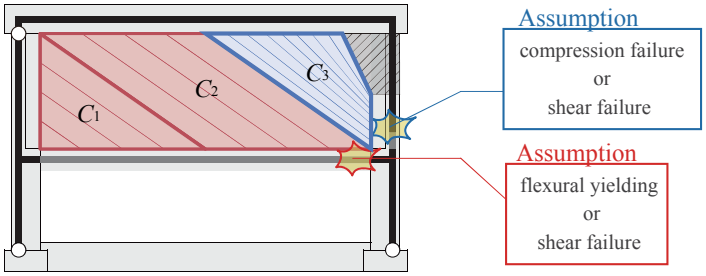

Figure 4.1. Failure mechanism

Figure 4.2 shows the structural models based on the experimental results and the shear failure area. The compression strut of the hatch area in Fig. 4.2 (a) and (b) is not considered in the evaluation to the shear strength of the wall, because the compression force is assumed little from the crack patterns at the peak of the shear strength during the positive loading (Fig. 3.4). It is assumed that shear failure occur at the area shown in Fig. 4.2(c), because the compression force of the wall panel above the column in the first story is included in the compression force of C_3 in this structural model. A method to evaluate the strength of the shear wall using these models is proposed based on the following assumptions.

1) The angles of C_1 and C_2 struts are defined as Eqn. (4.1).

$$\tan\theta_1 = \frac{H}{L/2} \tag{4.1}$$

where H is height of the shear wall and L is length of the boundary beam. However, if H is larger than $L/2$, it is assumed that θ_1 is 45 degrees. The angle of C_3 strut is assumed to be the angle θ_2 connected the H/4 from the bottom of the boundary column and the center of C_3 strut area. These are assumed from the crack patterns at the peak of the shear strength during the positive loading (Fig. 3.4).
2) The boundary beam is deformed by two struts and all vertical reinforcement in shear wall panel yielded. This is assumed from the tensile strains of the wall panel at the peak of the shear strength during the positive loading (Fig. 3.6).
3) It is assumed that the right end of the boundary beam is fixed support, because clockwise rotational deformation of the right corner is confined by the wall panel during the positive loading. It is assumed that the left end of the boundary beam is pinned support, because the clockwise rotational deformation of the left corner is unconfined during the positive loading (see Fig.4.3 d).

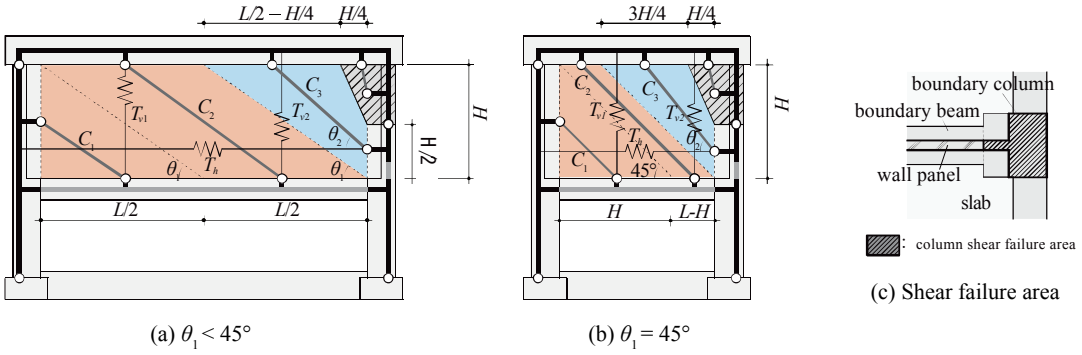

Figure 4.2. Structural model and column shear failure area

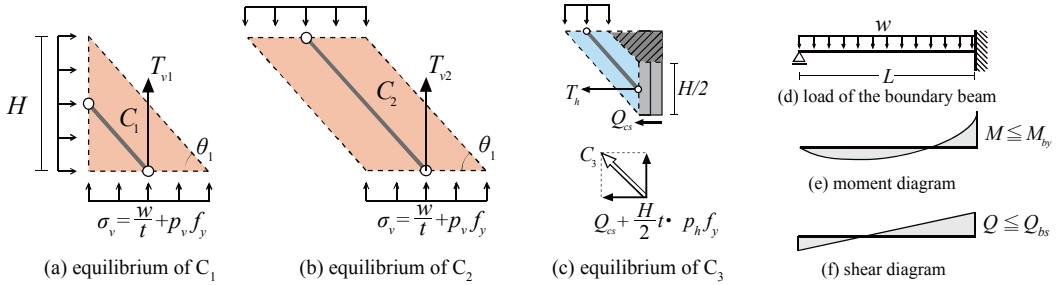

Figure 4.3. Equilibrium of compression struts and load of the boundary beam

Compression forces of C_1 and C_2 at the peak of the shear strength during the positive loading are computed based on the equilibrium of vertical stresses (Fig. 4.3 a and b). The value of w_{by} is the distributed load which causes flexural yielding at the corner of the boundary beam and is defined as Eqn. (4.2).

$$w_{by} = \frac{8M_{by}}{L^2} \tag{4.2}$$

where M_{by} is moment at flexural yielding of the boundary beam.
And, the value of w_{bs} is the distributed load which causes shear failure at the corner of the boundary beam and is defined as Eqn. (4.3).

$$w_{bs} = \frac{8}{5L} \cdot Q_{bs} \tag{4.3}$$

where Q_{bs} is shear strength of the boundary beam.
Additionally, the equilibrium of the vertical stresses of C_1 and C_2 (Fig. 4.3 a and b) leads to the following equation.

$$w/t = \sigma_v - p_v f_y \tag{4.4}$$

where p_v is ratio of the vertical reinforcement in the wall panel, t is thickness of the wall panel and σ_v is vertical component of compressive stresses of C_1 and C_2.
The equations (4.2), (4.3) and (4.4) lead to the equation to compute the vertical component of compressive stresses of C_1 and C_2.

$$\sigma_v = \frac{8M_{by}}{L^2 t} + p_v f_y \tag{4.5}$$

$$\sigma_v = \frac{8Q_{bs}}{5Lt} + p_v f_y \tag{4.6}$$

The compressive forces of C_1 and C_2 are calculated using the smaller value of the σ_v computed with equations (4.5) and (4.6) and are defined as Eqns. (4.7) and (4.8).

$$C_1 = \frac{1}{\sin\theta_1} \cdot \sigma_v \cdot \frac{H}{\tan\theta_1} \cdot t \tag{4.7}$$

$$C_2 = \frac{1}{\sin\theta_1} \cdot \sigma_v \cdot \left(L - \frac{H}{\tan\theta_1} \right) \cdot t \tag{4.8}$$

The compression strut C_3 is calculated based on the assumption shown by the blue color in Fig. 4.1. If compression failure occurs at the corner area of the wall panel, the compression strut C_3 is defined as Eqn. (4.9).

$$C_3 = \frac{H}{2} t \cdot \gamma_c F_c \cos\theta_2 \tag{4.9}$$

where γ_c is the reduction coefficient of the concrete strength based on Collins et al. (1990) and F_c is the concrete strength. If shear failure occurs at the boundary column, the compression strut C_3 is defined as Eqn. (4.10).

$$C_3 = \frac{Q_{cs} + (H/2)t \cdot p_h f_y}{\cos\theta_2} \tag{4.10}$$

where Q_{cs} is the shear strength of the shear failure area in Fig. 4.2(c) based on Kabeyasawa et al. (2007) and p_h is ratio of the horizontal reinforcement in the wall panel. The compressive force of C_3 is calculated using the smaller value computed with Eqns. (4.9) and (4.10).

In this method, the strength of the shear wall is considered as the summation of the horizontal components of the three struts and is defined as Eqn. (4.11).

$$Q_u = (C_1 + C_2)\cos\theta_1 + C_3 \cos\theta_2 \tag{4.11}$$

where Q_u is the strength of the shear wall.

Finally, the equation to compute the strength of the shear wall is defined as Eqn. (4.14) by substituting the Eqns. (4.5) ～ (4.10) in the Eqn. (4.11).

$$Q_u = \frac{1}{\tan\theta_1} \cdot \min\left(\frac{8M_{by}}{L}, \frac{8Q_{bs}}{5}\right) + \frac{Lt \cdot p_v f_y}{\tan\theta_1} + \min\left(\frac{H}{2} t \cdot \gamma_c F_c \cos^2\theta_2 \, , \, Q_{cs} + \frac{H}{2} t \cdot p_h f_y\right) \tag{4.12}$$

Table 4.1 shows the calculation results. The calculated shear strength and failure mode by using the proposed method are shown by gray color. The calculated shear strengths are within ± 30% of the observed strengths and the calculated failure modes agree with the observed failure modes in LB-0.90-4.3 and LB-0.23-2.3.

Table 4.1. Calculation results

	C_1 and C_2 (kN)			C_3 (kN)		calculation strength(kN)				experimental failure mode	maximum strength (kN)	Qu_{cal}/Qu_{exp}
	$\frac{8M_{by}}{L\tan\theta_1}$	$\frac{8Q_{bs}}{5\tan\theta_1}$	$\frac{Lt \cdot p_v f_y}{\tan\theta_1}$	$\frac{H}{2} t \cdot \gamma_c F_c \cos^2\theta_2$	$\frac{H}{2} t \cdot p_h f_y + Q_{cs}$	FS	FC	SC	SS			
LB-0.45-4.3	407	505	686	432	83 + 460	1636	1525	1623	1734	FS	1560	0.98
LB-0.90-4.3	407	505	1373	453	83 + 439	2301	2232	2330	2399	FC	2350	0.95
LB-0.23-2.3	635	540	106	351	83 + 489	1313	1093	997	1217	SC	1170	0.85
SB-0.23-2.3	201	259	106	394	83 + 493	883	701	759	941	SC	990	0.71

5. CONCLUSIONS

1. The strength of the shear wall located above an open frame is improved by increasing vertical reinforcement in the wall and size of the boundary beam in second story.

2. In the long-span specimens, flexural yielding occurred at the boundary beam in the second story. On the other hand in the short-span specimens, shear failure occurred at the boundary beam in the second story.

3. The effect of the vertical reinforcement on the shear strength of wall located above an open frame is larger than that of the boundary beam. Therefore, increasing vertical reinforcement in the wall panel can be equivalent with increasing the rigidity of the boundary beam.

4. In this research, a method using three compression struts is proposed. The calculated shear strengths by using the proposed method agree with the observed strengths.

AKCNOWLEDGEMENT
This work was financially supported by the Ministry of Land, Infrastructure, Transport and Tourism.

REFERENCES

Building Center of Japan (2007), "*Structural Guidelines for Building Structures*" BCJ (in Japanese)
Kabeyasawa T. Kabeyasawa T. (2007), "Practical Shear Design Equations for Reinforced Concrete Column with a Wing Wall" *Proceedings of the 5th Annual Meeting of Japan Association for Earthquake Engineering*, pp.115-120 (in Japanese)
Michael P. Collins and Denis Mitchell (1990), "*Prestressed Concrete Structures*" Prentice-Hall